Cell, Vol. 121, 725–737, June 3, 2005, Copyright ©2005 by Elsevier Inc. DOI 10.1016/j.cell.2005.04.030

Cryptic Pol II Transcripts Are Degraded by a Nuclear Quality Control Pathway Involving a New Poly(A) Polymerase

Françoise Wyers,[4,5,7] Mathieu Rougemaille,[5,7] Gwenaël Badis,[1] Jean-Claude Rousselle,[2] Marie-Elisabeth Dufour,[4] Jocelyne Boulay,[5] Béatrice Régnault,[3] Frédéric Devaux,[6] Abdelkader Namane,[2] Bertrand Séraphin,[2,5,*] Domenico Libri,[5,*] and Alain Jacquier[1,*]

[1]Unité de Génétique des Interactions Macromoléculaires
CNRS-URA2171-Institut Pasteur
[2]PT "Proteomique"
CNRS-URA2185-Institut Pasteur
[3]PT "Puces à ADN"
Institut Pasteur
25 rue du Docteur Roux
75724 Paris Cedex 15
[4]Equipe Labelisée La Ligue
[5]Centre de Génétique Moléculaire
CNRS-UPR2167
Avenue de la Terrasse
91190 Gif sur Yvette
[6]Laboratoire de Génétique Moléculaire
Ecole Normale Supérieure
CNRS-UMR 8541
46 rue d'Ulm
75005 Paris
France

Summary

Since detection of an RNA molecule is the major criterion to define transcriptional activity, the fraction of the genome that is expressed is generally considered to parallel the complexity of the transcriptome. We show here that several supposedly silent intergenic regions in the genome of *S. cerevisiae* are actually transcribed by RNA polymerase II, suggesting that the expressed fraction of the genome is higher than anticipated. Surprisingly, however, RNAs originating from these regions are rapidly degraded by the combined action of the exosome and a new poly(A) polymerase activity that is defined by the Trf4 protein and one of two RNA binding proteins, Air1p or Air2p. We show that such a polyadenylation-assisted degradation mechanism is also responsible for the degradation of several Pol I and Pol III transcripts. Our data strongly support the existence of a posttranscriptional quality control mechanism limiting inappropriate expression of genetic information.

Introduction

Most, if not all, eukaryotic primary transcripts, whether transcribed by RNA polymerase (Pol) I, II, or III, undergo maturation, which includes endonucleolytic severing, exonucleolytic trimming, splicing, nucleotide modifications/edition, and/or capping. Interestingly, most mature 3′ ends are generated by processing. Some result from cleavage and/or trimming, while others are extended by polymerases of the β family, which add 3′ tails without the help of a DNA template: CCA for tRNA (Schurer et al., 2001) or poly(A) sequences for mRNA (Proudfoot and O'Sullivan, 2002). Addition of poly(A) tails to mRNAs occurs at an endonucleolytic cleavage site that is severed cotranscriptionally. The Pap1p protein has poly(A) polymerase activity but depends on the assembly of a large complex for its function, which also insures correct positioning and control the length of the poly(A) tail (Keller and Minvielle-Sebastia, 1997). In eucaryotes, polyadenylation of coding RNAs has at least three important functions: it is required for RNA stability, efficient nucleocytoplasmic export, and translation. Except for a limited number of exclusively nuclear species, most transcripts reach the cytoplasm, where a large majority contribute to protein synthesis.

In this canonical view of the RNA synthesis pathway, the expressed fraction of the genome in a given cell is determined by accurate promoter selection. Transcription from these landmarks generates primary transcripts that are matured into functional RNA molecules, while the remaining fragments of the primary transcripts (e.g., introns, 3′ trailers, as well as 3′ extensions and internal spacers of the pre-rRNAs and pre-tRNAs) are rapidly degraded (e.g., Kim et al. [2004], West et al. [2004]). These events may explain the high rate of degradation of a fraction of nuclear RNAs never reaching the cytoplasm (e.g., Egyhazi [1976]). In addition to degradation events targeting short-lived processing intermediates, specific nuclear RNA decay pathways also destroy aberrant pre-mRNAs or those failing to be exported (Bousquet-Antonelli et al., 2000; Das et al., 2003; Libri et al., 2002; Torchet et al., 2002). In yeast, Rat1p and the exosome are two exonucleases implicated in these nuclear degradation processes: Rat1p is a 5′–3′ exonuclease showing sequence similarity to Xrn1, the major 5′–3′ exonuclease involved in cytoplasmic mRNA decay (Johnson, 1997). Rat1p is mostly nuclear and has been implicated in the maturation of pre-rRNAs and snoRNAs (Petfalski et al., 1998) and in transcription termination (Kim et al., 2004). The exosome is a large complex of 3′–5′ nucleases that is found both in the nucleus and in the cytoplasm (Mitchell and Tollervey, 2000). The nuclear form of the complex contains two specific subunits, Rrp6p and Lrp1p, that are its only nonessential subunits. The exosome has been implicated in numerous nuclear RNA processing and degradation events including pre-rRNA and sn(o)RNA maturation (Allmang et al., 1999a; Petfalski et al., 1998) and the turnover of pre-mRNAs in processing/splicing and RNA export mutants (Bousquet-Antonelli et al., 2000; Das et al., 2003; Libri et al., 2002; Torchet et al., 2002). Presence of both Rat1p and exosome homologs in eukaryotic species suggests that the cognate decay pathways are evolutionarily conserved.

*Correspondence: bertrand.seraphin@cgm.cnrs-gif.fr (B.S.); dominico.libri@cgm.cnrs-gif.fr (D.L.); jacquier@pasteur.fr (A.J.)
[7]These authors contributed equally to this work.

To identify new targets for the nuclear exosome, we have analyzed the transcriptome of a strain lacking Rrp6p with DNA microarrays. In accordance with previous studies, polyadenylated forms of numerous Pol II and Pol III noncoding RNAs (Allmang et al., 1999a; Kadaba et al., 2004; van Hoof et al., 2000) and of transcripts derived from the rDNA locus (Kuai et al., 2004) accumulated. Surprisingly, we identified in addition new polyadenylated transcripts mapping to intergenic regions. These were characterized as novel Pol II transcription units. Accumulation of the cognate RNAs in a *rrp6* mutant results from their stabilization rather than from transcriptional activation. Interestingly, most poly(A) additions to these transcripts are not mediated by the classical polyadenylation machinery. Database searches revealed the presence of other potential poly(A) polymerases encoded by the yeast genome, including Trf4p that has recently independently been shown to be required for polyadenylation and degradation of hypomodified forms of tRNAmet (Kadaba et al., 2004). Consistently, we show that Trf4p associates with Air1p and Air2p to form a new enzyme endowed with polyadenylation activity. This complex associated with Mtr4p, a putative RNA helicase previously implicated in activation of the nuclear exosome (de la Cruz et al., 1998; Liang et al., 1996). Most importantly, the polyadenylation of most cryptic transcripts derived from intergenic regions detected in the *rrp6Δ* background was nearly completely abolished in the absence of Trf4p, leading to their further stabilization. Taken together, these results demonstrate that a novel yeast nuclear poly(A) polymerase is implicated in a quality control process targeting numerous RNA to degradation by the exosome. Notably, this mechanism appears to limit the genomic noise resulting from inappropriate transcription of intergenic regions in the genome. These observations have several evolutionary implications.

Results

New Cryptic Transcripts Accumulate in the Absence of Rrp6p

The role of the Rrp6p exonuclease in the nuclear turnover of Pol II transcripts is still unclear. To identify new Rrp6p targets, we compared the transcriptomes of an *rrp6Δ* and a wild-type strain using Affymetrix DNA microarrays spanning the entire yeast ORFeome as well as some noncoding RNAs and intergenic regions. Two microarrays were used with RNAs from a wild-type strain (BMA64; see Table S1 in the Supplemental Data available with this article online) and two with RNAs from an *rrp6Δ* strain (LMA164), and the signal intensities were compared (Figure 1A). Importantly, the fluorescent probes were generated from total RNAs using oligo(dT) as primer and were thus enriched for probes against polyadenylated RNAs. While the vast majority of the cellular ORF-containing transcripts did not differ between the two strains (only 5.1% of verified ORFs reproducibly exhibit an *rrp6Δ*/WT ratio >2), a number of signals increased significantly in the *rrp6* mutant compared to the wild-type. Signals corresponding to almost all snRNAs and snoRNAs and directly downstream sequences strongly increased in an *rrp6Δ* background (red dots, Figure 1A), presumably as a consequence of the previously reported polyadenylation of such transcripts in the absence of Rrp6p (Allmang et al. [1999a], Allmang et al. [1999b], van Hoof et al. [2000], and see below). Likewise, signals corresponding to several rRNA species increased dramatically (yellow dots, Figure 1A), consistent with the reported stabilization of polyadenylated forms of these transcripts in *rrp6* mutants (Kuai et al. [2004] and see below; van Hoof et al. [2000]). Surprisingly, a number of signals derived from intergenic regions not linked to previously reported transcripts were also specifically enhanced in the *rrp6* mutant. Many of these signals corresponded to intergenic regions containing SAGE tags (Velculescu et al., 1997) (green dots, Figure 1A). Some (20.3%) of these SAGE probes (cured for those overlapping or next to known noncoding RNAs; see Table S3) reproducibly exhibited an *rrp6Δ*/WT ratio >2 in the two independent experiments (by comparison, only 0.8% of these probes exhibited a ratio >2 in the controls where the isogenic strains, i.e., WT-1/WT-2 and *rrp6Δ-1*/*rrp6Δ-2*, were compared). Similarly, 7.7% of these probes reproducibly exhibited an *rrp6Δ*/WT ratio >3 in both independent experiments when this number was only 0.9% for the verified ORFs. This specific behavior of the SAGE probes did not result from a bias in the distribution of signal intensities between the two types of features (SAGE probes versus ORFs), since essentially identical results were obtained when comparing a subset of ORF and SAGE probes exhibiting an average signal ratio within the same intensity class (300–3000 average intensities). The peculiarity of SAGE probes was also apparent when comparing the class frequencies distribution of log2-transformed ratios between the two kind of features (Figure 1B): the *rrp6Δ* versus wild-type ratios (green curves) appear more significantly shifted toward higher values relative to the control experiments (gray curves) for the intergenic SAGEs compared to verified ORFs.

These microarray results were confirmed by real-time PCR performed on cDNAs primed with sequence specific oligonucleotides (Figure 1C), indicating that, in at least six out of eight test regions, signal increase resulted from higher transcript amounts rather than from polyadenylation of a preexisting RNA. These new regions thus differ from loci containing noncoding RNAs (snRNAs, snoRNAs, rRNAs, etc.). Oligo-directed RNase H cleavage and Northern blots performed for four of these transcripts, corresponding to Affymetrix features *NEL025c* (Figure 2A), *NBL001c*, *NPL040w*, and *NGR060w* (Figure S1), revealed that they consisted in RNAs of heterogeneous sizes (250–600 nt). The oligo-directed RNase H cleavage experiments showed that, except for *NPL040W*, these transcripts had a discrete 5′ end, and their heterogeneity thus resulted from multiple 3′ ends. We chose *NEL025C* (located on chromosome V between *RMD6* and *DLD3*) for further studies. RNaseH cleavage with oligo dT increased mobility of *NEL025c* transcripts but did not abolish size heterogeneity (Figure 2A, compare lanes 7 and 8). The polyadenylation status of these heterogeneous transcripts was further confirmed by oligo-dT affinity selection (Figure 2B). Taken together, these data indicate that these transcripts extend from a defined 5′ end to multiple, closely

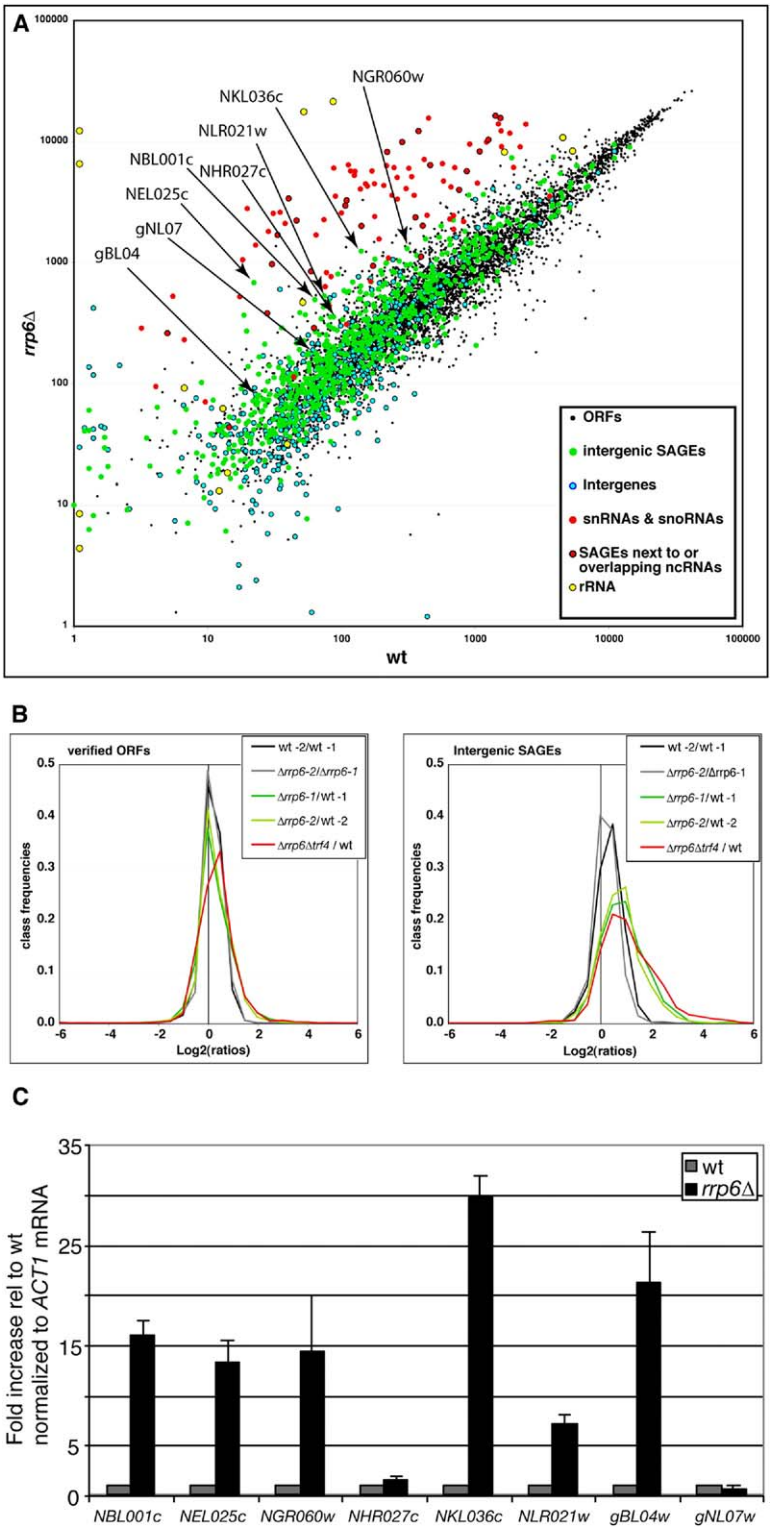

Figure 1. Genome-Wide Expression Profile of *rrp6Δ* Mutant versus Wild-Type

(A) Dot plot of signal intensities (average differences between perfect-match and mismatch oligonucleotides [Affymetrix MAS4.0 software], logarithmic scale) in wild-type (x axis) and *rrp6Δ* strain (y axis). Different classes of transcripts are color coded as indicated on the figure. The "SAGEs next to or overlapping ncRNAs" class represents features that were initially defined as intergenic SAGEs but that we found overlapping or directly juxtaposed to known noncoding RNAs—essentially snRNAs and snoRNAs; see Table S3). Arrows and labels point to dots corresponding to features that were analyzed by RT-PCR in Figure 1C.

(B) Distribution (class frequencies, one-third unit increments) of log2 transformed ratios (fold changes determined by the Affymetrix MAS4.0 software). Four microarrays were hybridized, two using RNAs from *RRP6* wild-type strains (BMA64) and two using RNAs from *rrp6Δ* strains (LMA164, see Table S1). The figure shows results obtained for the comparisons between wild-type-1 over wild-type-2 (black) or *rrp6Δ*-1 over *rrp6Δ*-2 (gray, controls) and *rrp6Δ*-1 over wild-type-1 or *rrp6Δ*-2 over wild-type-2, orange for verified ORFs and green for intergenic SAGE probes. Only verified ORFs (i.e., features defined as "ORF, verified" in the *Saccharomyces* Genome Database, www.yeastgenome.org) were taken into account in order to avoid statistical bias due to misannotated ORFs that should rather be classified as "intergenic features." Intergenic SAGE probes are as defined in the yeast S98 Affymetrix microarray and were cured for probes overlapping or directly next to known noncoding transcripts (see Table S3).

(C) The histogram shows the results of real-time PCR analysis after reverse transcription with specific oligonucleotides for eight arbitrarily chosen intergenic transcripts exhibiting a 3- to 30-fold signal increase in the *rrp6Δ* versus wild-type microarrays experiments (see Figure 1A). RNA amounts normalized to *ACT1* mRNA were expressed relative to the wild-type. Error bars were calculated from three independent experiments and represent standard deviations.

spaced 3′ ends to which poly(A) tails have been added. The oligo-dT-selected RNAs were also hybridized with a probe specific for the *NGR060W* transcripts and showed that these RNAs are also polyadenalylated in the *rrp6Δ* strain (data not shown).

Cryptic Transcripts Define New Pol II Transcription Units

Given their structure, we assessed whether *NEL025c*-derived RNAs are independent Pol II transcripts or readthrough products from neighboring genes. Immu-

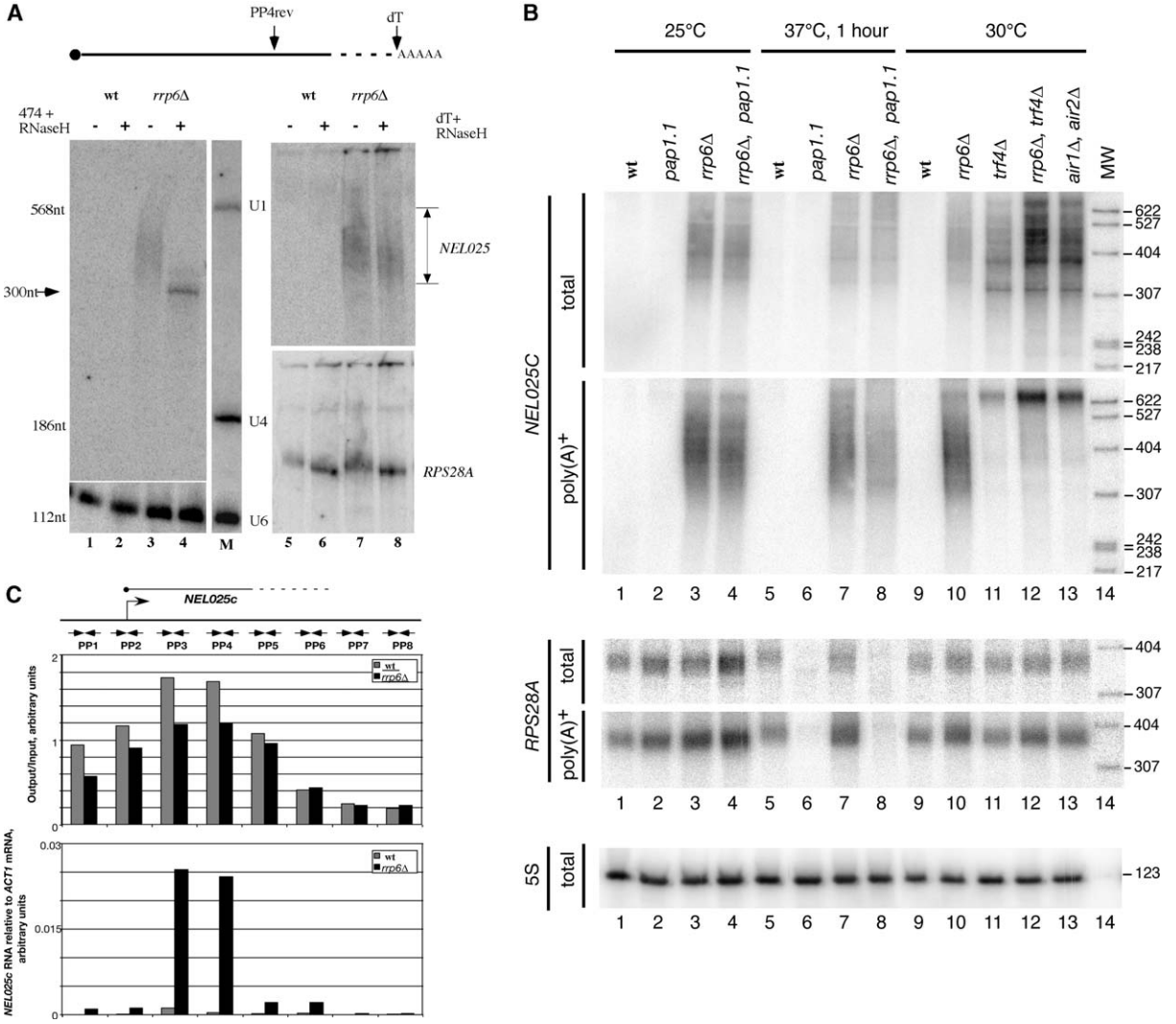

Figure 2. Characterization of the *NEL025C* Transcripts

(A) Northern blot characterization of the transcripts from the *NEL025C* region. Total RNAs from wild-type (lanes 1, 2, 5, and 6) or *rrp6Δ* (lanes 3, 4, 7, and 8) strains were separated on a 5% denaturing polyacrylamide gel. RNAs were treated with RNaseH in the presence of oligonucleotide P4rev (Table S2, lanes 2 and 4) or oligo-dT (lanes 6 and 8). The positions of the randomly primed double-strand DNA probe and oligonucleotide P4rev relative to the *NEL025c* RNA are indicated. After hybridization with the *NEL025c* probe, the filter on the right panel was stripped and rehybridized with a probe against the *RPS28A* mRNA for oligo-dT RNaseH cleavage control. Detection of U1, U4, and U6 snRNAs was used for loading control and size markers.

(B) Analysis of the polyadenylation status of *NEL025c* transcripts in different genetic backgrounds. Total RNAs (total) or oligo-dT-selected RNAs (poly[A]$^+$) were analyzed by Northern blots after separation on a 5% denaturing polyacrylamide gel and hybridization with a *NEL025c* random primed probe as in (A) (top panels). (Lanes 5–8) Cell cultures were shifted to 37°C for 1 hr prior to RNA extraction in order to inactivate Pap1p in the *rrp6Δ/pap1-1* strain. The filters used in the *NEL025c* panels were stripped and probed for *RPS28A* RNA as a control for Pap1p inactivation (*RPS28A* panels) and 5S RNA for loading control.

(C) Pol II occupancy (upper panel) in the *NEL025c* region in a wild-type (gray) and *rrp6Δ* strain (black). Chromatin immunoprecipitation (ChIP) was performed with an anti-Rpb1 antibody, and the DNA was analyzed by real-time PCR (top panel) with oligonucleotides spanning the entire region (primer pairs PP1–PP8, see Table S1) as schematized on top of the figure. RNAs were analyzed in parallel with the same primer pairs (bottom panel) by real-time RT-PCR.

noprecipitation with anti-cap antibodies (H20, kind gift of R. Lührmann) indicated that these transcripts are capped, which is a distinctive feature of Pol II transcripts and a specific mark of the transcription initiation site (Figure S2). Furthermore, inactivation of Pol II in a double mutant *rrp6Δ/rpb1-1*, expressing a thermosensitive form of the largest Pol II subunit (Nonet et al., 1987) and grown at nonpermissive temperature (37°C), resulted in the strong reduction of *NEL025c* transcript levels compared to a Pol III 5S ribosomal RNA control (Figure S3A). A similar result was also obtained for other intergenic transcripts (Figure S3B). Finally, the *NEL025c*-transcribed sequences expressed from their genomic locus but under the control of a heterologous

Pol II promoter (tetO7 operators under the control of the tetracycline repressible tTA transactivator; Gari et al. [1997]) were also strongly upregulated (~15 fold) in the absence of Rrp6p (Figure S3C). Together, these results indicate that these *rrp6Δ*-induced intergenic RNAs are independent, capped, and polyadenylated Pol II transcripts.

Cryptic Transcripts Are Unstable in Wild-Type Strains

To demonstrate that these intergenic RNAs are produced in both the wild-type and the *rrp6Δ* strain but have higher turnover rates in the former strain, we assessed Pol II occupancy at the *NEL025c* locus by chromatin immunoprecipitation (ChIP) in both strains. Real-time PCR analysis of the DNA immunoprecipitated with anti-Rpb1p antibodies was performed with primer pairs spanning the whole *NEL025c* locus. RNAs were analyzed in parallel by real-time RT-PCR with the same primer set. In striking contrast with the differences in transcript amounts, Pol II density was similar (or even slightly higher) in the wild-type strain compared to the *rrp6Δ* strain in the region tested (Figure 2C). This ChIP signal was specific since abolished by mutation of the largest Pol II subunit in an *rpb1-1* strain (Nonet et al., 1987; Schroeder et al., 2000) at the nonpermissive temperature (Figure S4). Pol II-ChIP analysis of other intergenic regions gave essentially identical results (data not shown). To further confirm that *NEL025c* transcripts are transcribed but more rapidly degraded in the presence of Rrp6p, we compared their turnover rates in a wild-type and *rrp6Δ* strains. Some *NEL025c* transcripts could be detected above background by real-time PCR in a wild-type strain, consistent with the existence of a SAGE tag in this genomic region (Velculescu et al., 1997). Use of an *rpb1-1* mutant (Nonet et al., 1987) allowed fast transcription shutoff in an otherwise wild-type or *rrp6Δ* context. As expected, the turnover rate of *NEL025c* transcripts was significantly higher in the *rpb1-1* strain compared to the *rpb1-1/rrp6Δ* strain, although the very low amount of transcripts in the *rpb1-1* strain precluded precise determination of the half-life of these RNAs (t1/2 <3 min in the *rpb1-1* strain and ~10 min in the *rpb1-1/rrp6Δ* strain); *ACT1* turnover rate was not significantly different in the two strains (Figure S5). Altogether, these data indicate that the *NEL025c* RNAs are produced in both the *rrp6Δ* and the wild-type strains, but, in the latter, the RNAs are more rapidly degraded. Degradation of these RNAs was also dependent on the integrity of the core exosome, as depletion of Rrp41p resulted in a similar stabilization of the *NEL025c* transcripts (Figure S6). Given the properties of the RNA products of these regions, revealed in the *rrp6Δ* strain, we named them CUTs for cryptic unstable transcipts.

NEL025c Transcripts Are Mainly Polyadenylated by a Pap1p-Independent Process

For most Pol II transcripts, the standard polyadenylation machinery adds poly(A) to a limited number of sites generated by cleavage. The heterogeneous 3′ ends of the CUTs were thus unexpected. To test the involvement of the standard polyadenylation machinery in *NEL025c* CUT poly(A) formation, we analyzed its polyadenylation status in an *rrp6Δ/pap1-1* double mutant shifted for 1 hr at the nonpermissive temperature (37°C). Oligo-dT-selected RNAs were analyzed by Northern blot (Figure 2B). Strikingly, Pap1p mutation did not strongly affect the amount and profile of the most abundant polyadenylated forms of these heterogeneous transcripts (300–400 nucleotides long), although the amount of the less abundant longest forms (>500 nucleotides) appear to decrease in the *rrp6Δ/pap1-1* strain compared to the *rrp6Δ* strain (Figure 2B, lanes 1–8). As a control, polyadenylation of *RPS28A* mRNA, a standard Pap1p substrate, was strongly inhibited in these conditions (Figure 2B). These observations suggested that the main polyadenylated forms of the *NEL025c* heterogeneous transcripts were polyadenylated by a machinery not involving Pap1p.

TRF4 Is the Catalytic Subunit of a Second Yeast Nuclear Poly(A) Polymerase

These results suggested the presence of at least another yeast poly(A) polymerase in addition to the classical machinery. Database searches revealed the presence of two highly related proteins, Trf4p and Trf5p, with distant similarity to Pap1p. These factors are similar to Cid1 and Cid13 from *S. pombe* and to Gld2 from *C. elegans* and related mammalian proteins that were recently described as cytoplasmic poly(A) polymerases (Kwak et al., 2004). While this work was in progress, a role for Trf4p in the polyadenylation of aberrant hypomodified $tRNA^{Met}$ was proposed (Kadaba et al., 2004).

To directly test whether Trf4p was endowed with poly(A) polymerase activity, we purified Trf4p and control factors from yeast using the TAP method (Rigaut et al., 1999) and assayed their poly(A) polymerase activity by following the incorporation of radiolabeled ATP in acid insoluble material using total yeast RNA as substrate. A strong incorporation was specifically detected with Trf4p-TAP (Figure 3A). In a similar assay, a Trf5p-TAP preparation was poorly active (data not shown). RNA polymerase activity of the Trf4p-TAP preparation is specific for ATP and could be primed by all tested substrates, including oligo(A) and tRNAs, with the exception of poly(U) (data not shown). Extension of an in vitro-transcribed RNA occurred in a time (data not shown) and Trf4-TAP concentration (Figure 3B) dependent manner in an apparent distributive reaction incorporating up to 500 residues. Mutation of two catalytic site residues (Wang et al., 2000) abolished the poly(A) polymerase activity of a Trf4-236-TAP preparation (Figure 3C). Overall, these data demonstrated the existence of a new yeast poly(A) polymerase having Trf4p as a catalytic subunit that we confirmed to be nuclear (Huh et al. [2003] and data not shown).

Air1p, or Air2p, Associates with Trf4p to Form Active Polymerases

While our results demonstrate that Trf4p is a subunit of a new poly(A) polymerase, recombinant Trf4-produced in *E. coli* was inactive in polyadenylation assays (see below), suggesting the requirement for additional factors and/or protein modification(s). Mass spectrometry

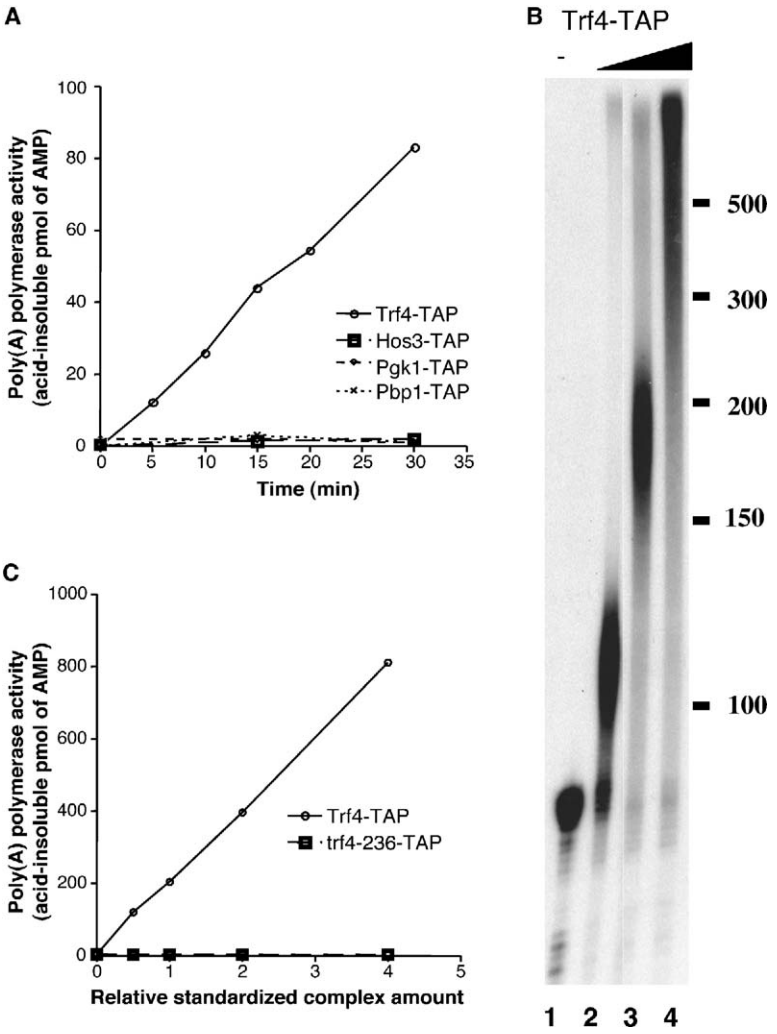

Figure 3. TRF4 Is a Subunit of a New Yeast Poly(A) Polymerase

(A) Incorporation of radioactive α32P-ATP into acid insoluble poly(A) was assayed in time course reactions using TAP-purified proteins and yeast RNA as substrate. Background activity was detected using TAP-purified Hos3, Pgk1, and Pbp1 control proteins. Identical quantities of the various proteins, as estimated from a Bradford assay, were used for each test.

(B) The polyadenylation activity associated with TRF4 and product length was tested by denaturing gel electrophoresis. An internally labeled RNA was used as substrate (lane 1) for a 30 min reaction. The product size observed at various concentrations of TAP-purified Trf4 complex was estimated by comparing with the migration of a single-stranded DNA marker (left, size in nucleotide).

(C) Mutation of the TRF4 catalytic center abolishes poly(A) polymerase activity. Incorporation of radioactive α32P-ATP into acid insoluble poly(A) in 30 min reactions was tested for TAP-purified wild-type trf4 and the trf4-236 mutant. Complex concentration was normalized by Western blotting using an antibody directed against Trf4 with concentration 0.5 corresponding to the quantity used in (A).

analysis of the purified Trf4p-TAP complex (Figure 4A) revealed the presence of additional factors, two of which that were identified as the related Air1 and Air2 proteins, which are located in the nucleus and have been previously implicated in nucleocytoplasmic mRNA transport (Inoue et al., 2000). A larger protein present at substoichiometric levels was identified as Mtr4p, a putative RNA helicase that was shown to interact functionally with the exosome (de la Cruz et al., 1998), supporting a role for Trf4p in the degradation of CUTs (see below). In addition, several ribosomal proteins were found in the purified fraction, possibly as a consequence of the implication of Trf4p in rRNA processing (see below). All these data are consistent with previous large-scale studies (Ho et al., 2002; Ito et al., 2001; Krogan et al., 2004). TAP purifications of Air1p-TAP and Air2p-TAP (Figure 4B) and the substoichiometric presence of either protein in the Trf4p-TAP preparations support the existence of two independent complexes containing either Air1p or Air2p associated with Trf4p.

Both Air1p-TAP and Air2p-TAP complexes were shown to be active in poly(A) synthesis (data not shown). The presence of either one of the two proteins is, however, required, as only in the absence of both Air1p and Air2p was the poly(A) polymerase activity abolished (Figure 4C).

Purified recombinant Air1p or Air2p failed to restore the activity of a recombinant Trf4p (Figure 4D). However, recombinant Air1p and Trf4p coexpressed in *E. coli* cells copurified with Trf4p, thus confirming a direct interaction. Most importantly, the resulting complex was active in polyadenylation (Figure 4D, a similar result was obtained for Air2-Trf4, data not shown). Thus, either Air1p or Air2p directly binds Trf4p, and these proteins are necessary and sufficient to form active polyadenylation enzymes.

Trf4 Is Required for the Polyadenylation and Degradation of the *NEL025c* Transcripts

To assess whether Trf4p plays a role in polyadenylation and/or degradation of *NEL025c* CUTs, we constructed strains deleted for *TRF4* in a wild-type or *rrp6Δ* background. The combination of the two mutations resulted in a strong synthetic growth impairment (see Figure S7), suggesting that Rrp6p and Trf4p are functionally linked.

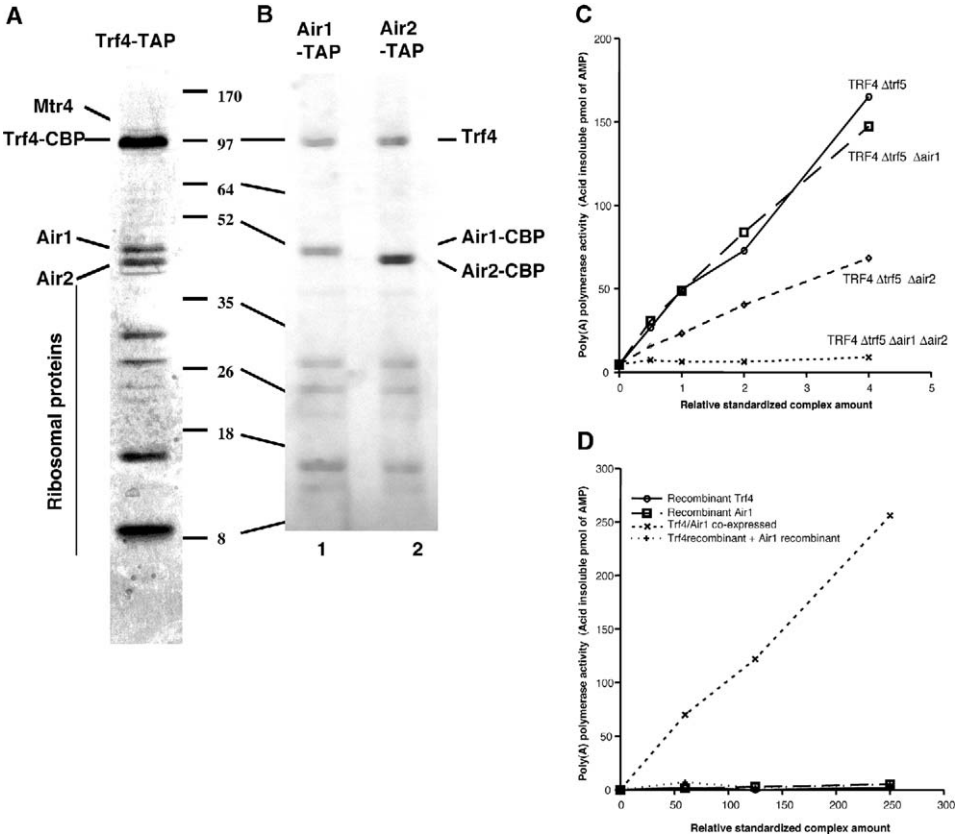

Figure 4. Trf4 Associates with Air1 or Air2 to Form an Active Poly(A) Polymerase

(A) A Coomassie blue-stained gel of proteins associated with TAP-purified Trf4p. Proteins identified by mass spectrometry are labeled. Position of migration of a molecular weight marker is indicated on the right.

(B) Proteins present in the TAP-purified fractions associated with Air1-TAP or Air2-TAP. Position of migration of the tagged proteins and Trf4 (identified by Western blotting) are indicated on the right, while the position of migration of a molecular weight marker is indicated on the left.

(C) Poly(A) polymerase activity requires Air1 or Air2. Concentration of the Trf4-TAP-purified complexes obtained from the strains of indicated genotypes were normalized by Western blotting using an antibody directed against Trf4. Poly(A) polymerase activity was assayed as described for Figure 3A.

(D) The poly(A) polymerase activity of recombinant Trf4, recombinant Air1, a mixture of both proteins, or a recombinant complex generated by coexpression of Trf4 and Air1 was tested. Protein concentration was normalized by Bradford assay.

To quantify the levels of both polyadenylated and nonadenylated transcripts in these strains, we first performed real-time PCR analyses after priming cDNA synthesis either with an oligonucleotide specific for *NEL025c* transcripts (total) or with oligo-dT (polyadenylated fraction) (Figure 5A). All data were normalized using *ACT1* mRNA levels. Strikingly, deletion of *TRF4* leads to stabilization of *NEL025c* transcripts (and other CUTs, Figure 5B and data not shown) to a level that is even higher than the one observed in an *rrp6*Δ strain. However, these transcripts appear to be mostly nonadenylated, in contrast to what was observed in the absence of Rrp6p (Figure 5A). Northern blot analysis confirmed that depletion of Trf4p resulted in a strong accumulation of *NEL025c* transcripts (Figure 2B, lane 11) as well as other CUTs (Figure S1). Note that, in the absence of *TRF4*, deletion of *RRP6* strongly enhances the accumulation of the *NEL025c* and other CUT transcripts, as shown both by quantitative RT-PCR and Northern blot analyses (Figures 5A, 5B, and 2B and Figure S1), suggesting that degradation of a fraction of these RNAs still occurs despite Trf4p absence. The most abundant *NEL025c* RNA species (~350 nt long) were absent from the oligo-dT selected fraction, in contrast to what was observed in the *rrp6*Δ single mutant strain, confirming that the polyadenylation of these transcripts is Trf4p dependent. In contrast, however, a larger polyadenylated product (enriched upon oligo-dT selection), of relative low abundance in the total RNA samples (Figure 2B, lane 12), was strongly stabilized in the absence of both Rrp6p and Trf4p. This polyadenylated transcript was completely absent from the oligo-dT selected fraction when Pap1p was inactivated, suggesting that it corresponds to a small fraction of *NEL025c* transcripts polyadenylated by the normal Pap1p-dependent machinery. Most interestingly, this polyadenylated RNA species accumulated only when both Rrp6p and Trf4p are absent, suggesting that, even though it might result from the normal, Pap1p-dependent, polyadenylation pathway, its precursor and/or itself are degraded by the coordinated actions of Rrp6p and Trf4p (see Discussion). In order to assess the generality of this observa-

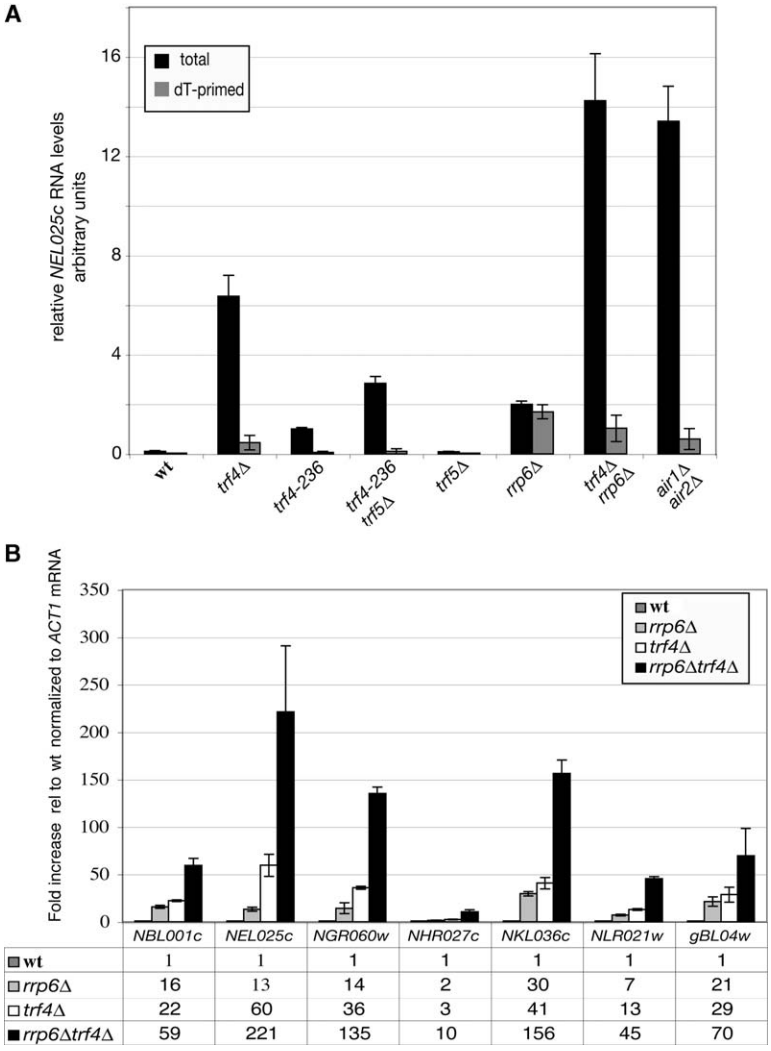

	NBL001c	NEL025c	NGR060w	NHR027c	NKL036c	NLR021w	gBL04w
wt	1	1	1	1	1	1	1
rrp6Δ	16	13	14	2	30	7	21
trf4Δ	22	60	36	3	41	13	29
rrp6Δtrf4Δ	59	221	135	10	156	45	70

Figure 5. Real-Time RT-PCR Analysis of CUTs in Mutants of the Trf4/Exosome Degradation Pathway

(A) Real-time RT-PCR analysis of *NEL025c* transcripts in mutants of the Trf4p/exosome degradation pathways. cDNA synthesis was performed with a specific oligonucleotide (total) or oligo-dT (dT-primed) before real-time PCR analysis with primer pair PP4. These signals are proportional to the total and polyadenylated fraction, respectively. Relative normalization was performed using *ACT1* mRNA as follows: the amount of every sample was divided by a normalization index representing the ratio between the *ACT1* value in that given sample and the average value of *ACT1* mRNA in all samples. The dT-primed/total ratio for *NEL025c* transcripts in a *rrp6Δ* strain was 0.87 ± 0.09 (n = 3), which is similar (although consistently higher) than the average dT-primed/total ratio for *ACT1* mRNA (0.65 ± 0.048; n = 24).

(B) Real-time RT-PCR analysis of other CUTs (same set as in Figure 1C) in *trf4Δ* and *trf4Δ/rrp6Δ* strains. The amount of each transcript in a given mutant strain is expressed relative to the amount in a wild-type strain. Average stabilization values are indicated in the panel below the histogram. Stabilization values in an *rrp6Δ* background are reported for comparison. In (A) and (B), error bars represent standard deviations calculated from three independent experiments.

tion, we analyzed with Affymetrix microarrays (which detect mainly polyadenylated species, as they use oligo-dT primed cDNAs), the global effect of the *rrp6Δ/trf4Δ* double deletion on the stabilization of such polyadenylated forms of CUTs. Figure 1B (red curves) shows that stabilization of these minor, Trf4p-independent, polyadenylated forms of CUTs is widespread, as the signals of a large number of intergenic SAGEs were enhanced in the double mutant relative to the wild-type. Finally, the depletion of Trf5 had no marked effect the amount of CUTs (Figure 5A and data not shown) or on the profiles of the oligo-dT-selected *NEL025c* transcripts (data not shown). These data indicate that Trf4p is involved in polyadenylation of CUTs and, together with Rrp6p, in their degradation.

The Trf4-Associated Poly(A) Polymerase Activity Is Required for CUT Degradation

Because the Trf4p complex is a poly(A) polymerase in vitro and because Trf4p is involved in polyadenylation and degradation of CUTs in vivo, we assessed whether the enzymatic activity of the complex is required for CUTs degradation. We asked first whether the poly(A) polymerase catalytic site mutant (*trf4-236*) would affect CUT stability. As shown in Figure 5A, non-adenylated *NEL025c* transcripts were readily detected in a *trf4-236* strain, although they were stabilized to a lower extent than upon *TRF4* deletion. This intermediate effect was paralleled by the growth of the *trf4-236* mutant strain that was less affected than the *trf4Δ* strain (Figure S7). Interestingly, deletion of the *TRF4* paralogue *TRF5* in the *trf4-236* strain led to a stabilization of *NEL025c* transcripts that was greater than the one observed in a *trf4-236* strain, strongly suggesting a role for Trf5p in CUT degradation when Trf4p is not fully functional (Figure 5A). To further confirm that the poly(A) polymerase activity of the Trf4 complex is involved in CUT degradation, we analyzed CUT levels in a strain lacking both Air1 and Air2, as both proteins were required for poly(A) polymerase activity (see above). Real-time RT-PCR (Figure 5A, and data not shown) and Northern blot analyses (Figure 2B and Figure S1) of CUTs in this strain revealed a strong stabilization of these RNAs. For *NEL025c*, only the largest transcript accumulated in a polyadenylated form (Figure 2B). Altogether, these results strongly suggest that the

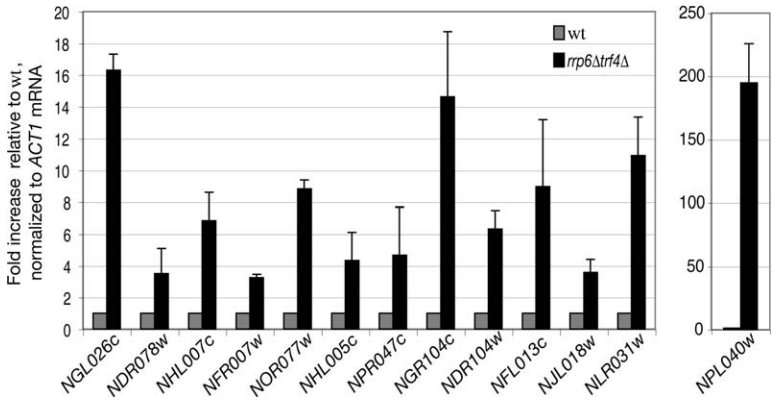

Figure 6. Most Intergenic Transcripts Are Stabilized in a *rrp6Δ/trf4Δ* Double Mutant

Real-time RT-PCR analysis in a *rrp6Δ/trf4Δ* strain of intergenic transcripts that exhibited a low *rrp6Δ*-dependent signal increase in the microarray experiments (ranging from 1.5- to 3.6-fold, 2.7-fold on average). Levels normalized to *ACT1* mRNA are expressed relative to the amount in a wild-type strain. Error bars were calculated from three independent experiments and represent standard deviations. Note that analysis for *NPL040w* is reported on a different scale, as this RNA is strongly stabilized in this strain.

poly(A) polymerase activity of Trf4p is associated with its role in CUT degradation.

Polyadenylation of rRNAs, snRNAs, and snoRNAs in an *rrp6Δ* Background Is Trf4p Dependent

Having established that Trf4p is involved in polyadenylation of CUTs, we tested whether the polyadenylated forms of the rRNAs, snRNAs, and snoRNAs observed in the *rrp6Δ* strain are also Trf4p dependent. Indeed, the presence of polyadenylated forms of U6, 5S, or 5.8S RNAs were dependent upon the presence of Trf4p (Figure 7 and data not shown). Inactivation of Pap1p had some effect on polyadenylation, in particular on the longest forms, but these effects were always weaker than the effect of *trf4Δ*. A similar observation was made for the snoRNA U18 (data not shown). Most importantly, the polyadenylated forms of these transcripts represent a small fraction of the total RNAs, and the absence of Trf4p had no strong influence on the amount of the mature forms of these transcripts (Figure 7), which is in sharp contrast with what we observed for CUTs.

Discussion

Our results support the existence of a quality control mechanism monitoring nuclear transcripts. This mechanism targets transcripts made by all three nuclear RNA polymerases. A characteristic feature of this process is the addition of poly(A) tail to the target molecules before their proper processing or degradation in an exosome-dependent manner

Numerous new RNA species accumulate in a *Δrrp6* strain. These include Pol I transcripts or derivatives thereof (e.g., 7S rRNA); Pol II transcripts, such as U18 snoRNA transcripts; and Pol III transcripts (e.g., species detected with the 5S probe). As previously reported (Allmang et al., 1999a; Kuai et al., 2004; van Hoof et al., 2000), we also found that a large fraction of these new species are polyadenylated in a *Δrrp6* strain but not in a wild-type strain. These poly(A)$^+$ species may represent normal processing intermediates with very short half-lives. Alternatively, they could represent nonfunctional transcripts targeted for degradation. Polyadenylation of such RNA species is unlikely to be restricted to *S. cerevisiae* and offers to cells a mean to control maturation or processing of these targets. Consistently, polyadenylated ribosomal RNAs were detected in the pathogenic fungi *Candida albicans* in a process controlled by the presence of serum (Fleischmann et al., 2004).

Although it has been reported (Kuai et al., 2004) that polyadenylation of several rRNA species in a *rrp6Δ* background depends on Pap1p integrity, our results only partially support this notion. In fact, Pap1p-dependent polyadenylation only accounts for a fraction of the polyadenylated rRNA species detected in *rrp6* mutants. This observation is paralleled by the analysis of snoRNA, snRNA, and CUTs. In most cases (e.g., for *NEL025c* and 5S RNAs), this fraction is minor compared to the fraction that is Trf4p dependent, and, most importantly, in no cases did mutation of Pap1p lead to stabilization of transcripts in a WT or *rrp6Δ* background. Currently, the significance of polyadenylation of these transcripts by Pap1p is unclear; it does not appear to stimulate their degradation, as shown here for Trf4p-dependent polyadenylation.

Another group of polyadenylated RNA accumulating in a *Δrrp6* strain corresponds to new cryptic Pol II transcripts. These CUT transcripts are present at extremely low concentration in wild-type cells, even though some of these transcripts were apparently detected by SAGE analyses (Velculescu et al., 1997). Nevertheless, they appear to represent bona fide transcripts generated by Pol II, containing a 5′ cap. These intergenic cryptic Pol II transcripts are usually relatively short and do not contain long or conserved reading frames. Thus, while we cannot formally exclude that they have a physiological role, their structure suggests that they result from the presence of adventitious promoters at random genomic locations. How widespread is the occurrence of cryptic intergenic transcription in the genome? We have confirmed by RT-PCR analysis that most if not all of the intergenic SAGE transcripts that exhibit an *rrp6Δ*/WT signal ratio >2 in the microrray experiments (roughly 20% of the total) are indeed responsive to mutation of the TRF4p/exosome degradation pathways. To assess whether intergenic SAGE transcripts exhibiting lower *rrp6Δ*/WT signal ratios are bona fide CUTs, we exploited the observation that, in a *trf4Δ/rrp6Δ* mutant, CUTs are stabilized to a higher level, which should improve sensitivity. Microarray analysis in this context was not informative, as stabilized CUTs are mostly non-

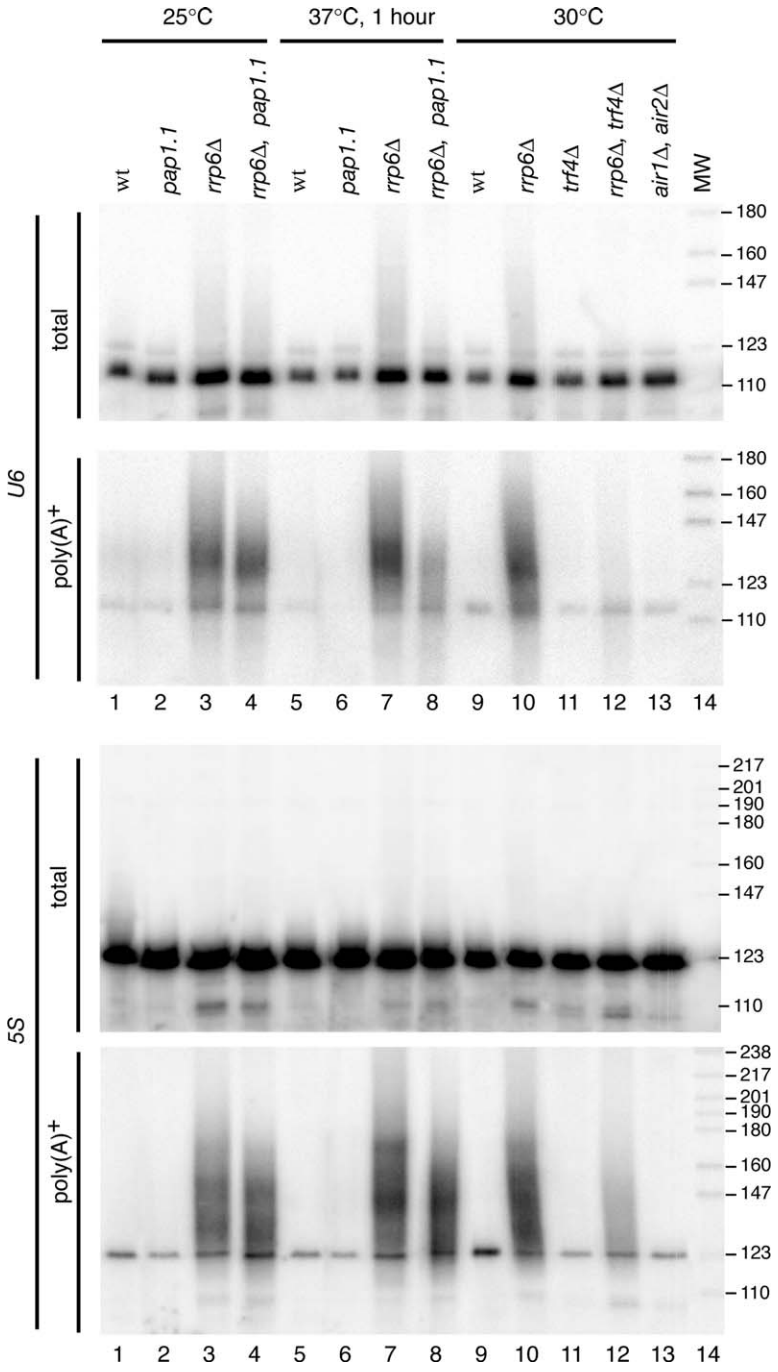

Figure 7. Analysis of the Polyadenylation Status of U6 and 5S rRNA in Different Genetic Backgrounds

As in Figure 2B, except that the filters were hybridized with [^{32}P]-labeled oligonucleotides specific for U6 snRNA (top panels) or 5S rRNA (bottom panels).

polyadenylated, while the standard Affymetrix technology only allows the detection of polyadenylated species (Figure 1B, red curves). We then extended RT-PCR analyses with sequence-specific primers to 13 additional intergenic SAGE regions that exhibited even a very modest, *rrp6Δ*-dependent signal increase in the microarray experiments (1.5- to 3.6-fold increase; 2.7-fold in average). Remarkably, all these RNAs species were responsive to the *trf4Δ/rrp6Δ* mutation (Figure 6), strongly suggesting that they are bona fide CUTs. This is consistent with the notion that a large fraction of the intergenic regions containing SAGE tag (more than 10% of the overall intergenic regions; Velculescu et al. [1997]) encode genuine transcripts that are normally targeted for degradation by the coordinated action of the nuclear exosome and the Trf4-associated complex. Consequently, as some intergenic transcripts might have escaped SAGE detection, a minimal genome-wide estimate of cryptic transcripts for all intergenic regions is likely to be more than 5%–10%. Thus, spurious intergenic transcription appears to be widely spread within the yeast genome. This is likely to be evolutionarily widespread. Indeed, microarray tiling experiments revealed the presence of numerous unsuspected tran-

scripts encoded by intergenic regions of mammalian chromosomes (Johnson et al., 2005). A relatively low specificity of promoter recognition might leave more flexibility for evolution and/or regulation. Thus, paralleling observations made with ribosome fidelity mutants (Ruusala et al., 1984), promoter recognition by the Pol II machinery may remain suboptimal. We suggest that, in addition to a chromatin-dependent repression of cryptic promoters usage, a parallel and/or overlapping strategy that involves a posttranscriptional quality control mechanism evolved to get rid of cryptic transcripts.

Our data demonstrate that Trf4 is a poly(A) polymerase. While Trf4 was previously suggested to be a DNA polymerase involved in DNA repair (Castano et al., 1996), we believe that these original data have to be reinterpreted, as its DNA polymerase activity is extremely weak compared to its poly(A) polymerase activity (Wang et al., 2000). Furthermore, Trf4 clearly affects polyadenylation in vivo, supporting the in vitro biochemical activity. Nevertheless, we cannot exclude that Trf4 has both activities. Identification of a second yeast nuclear poly(A) polymerase targeting RNA for degradation by the exosome must also be reconciled with the presence of poly(A) tails on (pre-)mRNA that are not degraded. How the cell discriminates between aberrant and functional transcripts remains unknown. Substituting the natural cryptic promoter by a heterologous one (Figure S3C) or inserting a bona fide terminator (data not shown) did not change the susceptibility of the *NEL025c* CUT toward Rrp6p.

What is the role of the Trf4p complex in recognition and degradation of unstable transcripts? Trf4p appears to have a role in CUT degradation (most likely through stimulation or targeting of the exosome) that is independent of its polyadenylation activity as the *trf4-236* point mutant, which completely lacks pol(A) polymerase activity in vitro and is much less affected than the *trf4Δ* mutant (Figure 5A and Figure S7). In at least some cases, Trf5p might substitute for Trf4p function, which is suggested by the stronger phenotype of a *trf4-236/trf5Δ* mutant compared to either single mutants (Figure 5A and Figure S7). If Air1p/Air2p were also required for Trf5p function (which is presently unclear), the stronger phenotype of *air1Δ/air2Δ* cells compared to *trf4Δ* might be explained by a concomitant impairment of both Trf4p and Trf5p activities. Finally, it is unclear whether Rrp6p and the core exosome have different roles in the degradation of CUTs. A distinct role might be consistent with the observation that the patterns and the polyadenylation status of *NEL025c* transcripts are similar but not identical in an *rrp6Δ* mutant and in the depletion of the Rrp41p core component.

Degradation of *NEL025c* transcripts might be paradigmatic for the Trf4p/exosome pathway. The long form of the *NEL025c* transcript (which might be the precursor of the shortest forms) is polyadenylated by Pap1p but degraded in a Trf4p-dependent manner (which is polyadenylation independent, as its abundance but not its polyadenylation status is affected by *TRF4* deletion). It is conceivable, for instance, that a polyadenylation-independent role of the Trf4p/Air complex in this case would be to target the exosome on CUTs or other substrates, maybe through Mtr4p, a reported constituent of the nuclear exosome that is also found associated with the Trf4/Air complex. The shorter 300–500 nt transcripts, on the contrary, would require prior polyadenylation by the Trf4/Air complex for subsequent efficient degradation. This might result from stalling of the exosome at secondary structures, which would require the secondary addition of Trf4p-dependent poly(A) tails to resume degradation. In the *rrp6Δ/trf4Δ* double mutant, the combination of compromised exosome activity and lack of the Trf4/Air complex would result in both a very inefficient targeting of the primary *NEL025c* transcript as well as inefficient removal of degradation intermediates. The role of Trf4p poly(A) polymerase activity would then be very similar to batcterial poly(A) polymerases that have been shown to facilitate mRNA degradation by the degradosome (Dreyfus and Regnier, 2002). Indeed, the group of D. Tollervey has recently found that the Trf4p-associated complex enhances the nuclear exosome activity in vitro (LaCava et al., 2005). In this vein, it is noteworthy that the degradosome is homologous to the eukaryotic exosomes (Aloy et al., 2002; Symmons et al., 2002). The existence of Trf4p and Airp homolgues in human and other species suggests that the poly(A)-stimulated 3′–5′ nuclear degradation/processing of RNA is conserved in all eucaryotes.

Experimental Procedures

Standard experimental procedures are given as Supplemental Data under the section Supplemental Experimental Procedures.

Microarray Analyses

Microarray hybridizations were performed using the Affymetrix Yeast Genome S98 Array using protocols described by Affymetrix, Inc. (Santa Clara, CA). Data were analyzed using Affymetrix Microarray Suite 4.0 software for the *rrp6Δ* results and Affymetrix Microarray Suite 5.0 for the *rrp6Δ, trf4Δ* results. Microarray data are accessible in the Gene Expression Omnibus database (http://www.ncbi.nlm.nih.gov/geo/) under the accession number GSE2579.

Poly(A) Polymerase Assay

Reactions (20 μl) contained 20 mM Tris-HCl (pH 7.6), 50 mM KCl, 17.5 mM MgCl2, 1 mM DTT, 0.2 mM EDTA, 100 μg/ml BSA, 10% glycerol, 0.5 mM ATP, (α32P) ATP (150–500 cpm/pmol) and 0.25 μg of substrate (total yeast RNA, poly[A] [250 nt], or oligo[A] [15 nt]). The reaction was started by the enzyme addition (2.5–50 ng of TAP-purified complexes or 50–400 ng of recombinant proteins), incubated at 30°C for 30 min, and stopped by addition of 0.5 ml of 10% TCA. The precipitate was collected on glass fiber filter, washed, and counted. Alternatively ^{32}P-labeled LucΔ RNA was used as substrate in reactions without (α32P)ATP.

Supplemental Data

Supplemental Data include seven figures, three tables, and Supplemental References and can be found with this article online at http://www.cell.com/cgi/content/full/121/5/725/DC1/.

Acknowledgments

We thank R. Lührmann for antibodies, R. Gallie for plasmid, T.H. Jensen and M. Rosbash for comments on the manuscript, David Tollervey for generously communicating unpublished results, and Kristell Wanherdrick from "Genopole Ile de France, Site de la Montagne Sainte Geneviève, Institut Curie, Paris" for performing early microarray hybridizations. Discussion and experimental input from our lab colleagues, particularly F. Lacroute, E. Kisseleva-Romanova, E. Kastenhuber, M. Minet, C. Torchet, C. Saveanu, and M. Fromont-Racine, were deeply appreciated. Work in the lab of B.S. was supported by La Ligue Contre le Cancer (Equipe Labelisée

2005), the CNRS (particularly Programme PGP 2003), and the Ministry of Research (ACI BCMS). Work in the lab of A.J. was supported by the EEC (grant RNOMICS, QLG2-CT-2001-01554) and the Ministry of Research (grant "Subventions puces Affymetrix"). Work in the lab of D.L. was supported by the CNRS. M.R. is a recipient of a fellowship from the Ministry of Research.

Received: January 10, 2005
Revised: March 25, 2005
Accepted: April 19, 2005
Published online: May 19, 2005

References

Allmang, C., Kufel, J., Chanfreau, G., Mitchell, P., Petfalski, E., and Tollervey, D. (1999a). Functions of the exosome in rRNA, snoRNA and snRNA synthesis. EMBO J. *18*, 5399–5410.

Allmang, C., Petfalski, E., Podtelejnikov, A., Mann, M., Tollervey, D., and Mitchell, P. (1999b). The yeast exosome and human PM-Scl are related complexes of 3′→5′ exonucleases. Genes Dev. *13*, 2148–2158.

Aloy, P., Ciccarelli, F.D., Leutwein, C., Gavin, A.C., Superti-Furga, G., Bork, P., Bottcher, B., and Russell, R.B. (2002). A complex prediction: three-dimensional model of the yeast exosome. EMBO Rep. *3*, 628–635.

Bousquet-Antonelli, C., Presutti, C., and Tollervey, D. (2000). Identification of a regulated pathway for nuclear pre-mRNA turnover. Cell *102*, 765–775.

Castano, I.B., Heath-Pagliuso, S., Sadoff, B.U., Fitzhugh, D.J., and Christman, M.F. (1996). A novel family of TRF (DNA topoisomerase I-related function) genes required for proper nuclear segregation. Nucleic Acids Res. *24*, 2404–2410.

Das, B., Butler, J.S., and Sherman, F. (2003). Degradation of normal mRNA in the nucleus of *Saccharomyces cerevisiae*. Mol. Cell. Biol. *23*, 5502–5515.

de la Cruz, J., Kressler, D., Tollervey, D., and Linder, P. (1998). Dob1p (Mtr4p) is a putative ATP-dependent RNA helicase required for the 3′ end formation of 5.8S rRNA in *Saccharomyces cerevisiae*. EMBO J. *17*, 1128–1140.

Dreyfus, M., and Regnier, P. (2002). The poly(A) tail of mRNAs: bodyguard in eukaryotes, scavenger in bacteria. Cell *111*, 611–613.

Egyhazi, E. (1976). Quantitation of turnover and export to the cytoplasm of hnRNA transcribed in the Balbiani rings. Cell *7*, 507–515.

Fleischmann, J., Liu, H., and Wu, C.P. (2004). Polyadenylation of ribosomal RNA by *Candida albicans* also involves the small subunit. BMC Mol. Biol. *5*, 17.

Gari, E., Piedrafita, L., Aldea, M., and Herrero, E. (1997). A set of vectors with a tetracycline-regulatable promoter system for modulated gene expression in *Saccharomyces cerevisiae*. Yeast *13*, 837–848.

Ho, Y., Gruhler, A., Heilbut, A., Bader, G.D., Moore, L., Adams, S.L., Millar, A., Taylor, P., Bennett, K., Boutilier, K., et al. (2002). Systematic identification of protein complexes in *Saccharomyces cerevisiae* by mass spectrometry. Nature *415*, 180–183.

Huh, W.K., Falvo, J.V., Gerke, L.C., Carroll, A.S., Howson, R.W., Weissman, J.S., and O'Shea, E.K. (2003). Global analysis of protein localization in budding yeast. Nature *425*, 686–691.

Inoue, K., Mizuno, T., Wada, K., and Hagiwara, M. (2000). Novel RING finger proteins, Air1p and Air2p, interact with Hmt1p and inhibit the arginine methylation of Npl3p. J. Biol. Chem. *275*, 32793–32799.

Ito, T., Chiba, T., Ozawa, R., Yoshida, M., Hattori, M., and Sakaki, Y. (2001). A comprehensive two-hybrid analysis to explore the yeast protein interactome. Proc. Natl. Acad. Sci. USA *98*, 4569–4574.

Johnson, A.W. (1997). Rat1p and Xrn1p are functionally interchangeable exoribonucleases that are restricted to and required in the nucleus and cytoplasm, respectively. Mol. Cell. Biol. *17*, 6122–6130.

Johnson, J.M., Edwards, S., Shoemaker, D., and Schadt, E.E. (2005). Dark matter in the genome: evidence of widespread transcription detected by microarray tiling experiments. Trends Genet. *21*, 93–102.

Kadaba, S., Krueger, A., Trice, T., Krecic, A.M., Hinnebusch, A.G., and Anderson, J. (2004). Nuclear surveillance and degradation of hypomodified initiator tRNAMet in *S. cerevisiae*. Genes Dev. *18*, 1227–1240.

Keller, W., and Minvielle-Sebastia, L. (1997). A comparison of mammalian and yeast pre-mRNA 3′-end processing. Curr. Opin. Cell Biol. *9*, 329–336.

Kim, M., Krogan, N.J., Vasiljeva, L., Rando, O.J., Nedea, E., Greenblatt, J.F., and Buratowski, S. (2004). The yeast Rat1 exonuclease promotes transcription termination by RNA polymerase II. Nature *432*, 517–522.

Krogan, N.J., Peng, W.T., Cagney, G., Robinson, M.D., Haw, R., Zhong, G., Guo, X., Zhang, X., Canadien, V., Richards, D.P., et al. (2004). High-definition macromolecular composition of yeast RNA-processing complexes. Mol. Cell *13*, 225–239.

Kuai, L., Fang, F., Butler, J.S., and Sherman, F. (2004). Polyadenylation of rRNA in *Saccharomyces cerevisiae*. Proc. Natl. Acad. Sci. USA *101*, 8581–8586.

Kwak, J.E., Wang, L., Ballantyne, S., Kimble, J., and Wickens, M. (2004). Mammalian GLD-2 homologs are poly(A) polymerases. Proc. Natl. Acad. Sci. USA *101*, 713–724.

LaCava, J., Houseley, J., Saveanu, C., Petfalski, E., Thompson, E., Jacquier, A., and Tollervey, D. (2005). RNA degradation by the exosome is promoted by a nuclear polyadenylation complex. Cell *121*, this issue, 713–724.

Liang, S., Hitomi, M., Hu, Y.H., Liu, Y., and Tartakoff, A.M. (1996). A DEAD-box-family protein is required for nucleocytoplasmic transport of yeast mRNA. Mol. Cell. Biol. *16*, 5139–5146.

Libri, D., Dower, K., Boulay, J., Thomsen, R., Rosbash, M., and Jensen, T.H. (2002). Interactions between mRNA export commitment, 3′-end quality control, and nuclear degradation. Mol. Cell. Biol. *22*, 8254–8266.

Mitchell, P., and Tollervey, D. (2000). Musing on the structural organization of the exosome complex. Nat. Struct. Biol. *7*, 843–846.

Nonet, M., Scafe, C., Sexton, J., and Young, R. (1987). Eucaryotic RNA polymerase conditional mutant that rapidly ceases mRNA synthesis. Mol. Cell. Biol. *7*, 1602–1611.

Petfalski, E., Dandekar, T., Henry, Y., and Tollervey, D. (1998). Processing of the precursors to small nucleolar RNAs and rRNAs requires common components. Mol. Cell. Biol. *18*, 1181–1189.

Proudfoot, N., and O'Sullivan, J. (2002). Polyadenylation: a tail of two complexes. Curr. Biol. *12*, R855–R857.

Rigaut, G., Shevchenko, A., Rutz, B., Wilm, M., Mann, M., and Seraphin, B. (1999). A generic protein purification method for protein complex characterization and proteome exploration. Nat. Biotechnol. *17*, 1030–1032.

Ruusala, T., Andersson, D., Ehrenberg, M., and Kurland, C.G. (1984). Hyper-accurate ribosomes inhibit growth. EMBO J. *3*, 2575–2580.

Schroeder, S.C., Schwer, B., Shuman, S., and Bentley, D. (2000). Dynamic association of capping enzymes with transcribing RNA polymerase II. Genes Dev. *14*, 2435–2440.

Schurer, H., Schiffer, S., Marchfelder, A., and Morl, M. (2001). This is the end: processing, editing and repair at the tRNA 3′-terminus. Biol. Chem. *382*, 1147–1156.

Symmons, M.F., Williams, M.G., Luisi, B.F., Jones, G.H., and Carpousis, A.J. (2002). Running rings around RNA: a superfamily of phosphate-dependent RNases. Trends Biochem. Sci. *27*, 11–18.

Torchet, C., Bousquet-Antonelli, C., Milligan, L., Thompson, E., Kufel, J., and Tollervey, D. (2002). Processing of 3′-extended read-through transcripts by the exosome can generate functional mRNAs. Mol. Cell *9*, 1285–1296.

van Hoof, A., Lennertz, P., and Parker, R. (2000). Yeast exosome

mutants accumulate 3′-extended polyadenylated forms of U4 small nuclear RNA and small nucleolar RNAs. Mol. Cell. Biol. *20*, 441–452.

Velculescu, V.E., Zhang, L., Zhou, W., Vogelstein, J., Basrai, M.A., Bassett, D.E., Jr., Hieter, P., Vogelstein, B., and Kinzler, K.W. (1997). Characterization of the yeast transcriptome. Cell *88*, 243–251.

Wang, Z., Castano, I.B., De Las Penas, A., Adams, C., and Christman, M.F. (2000). Pol kappa: A DNA polymerase required for sister chromatid cohesion. Science *289*, 774–779.

West, S., Gromak, N., and Proudfoot, N.J. (2004). Human 5′→3′ exonuclease Xrn2 promotes transcription termination at co-transcriptional cleavage sites. Nature *432*, 522–525.